Proc. CIBSE A: Building Serv. Eng. Res. Technol. 18(1) 7–16 (1997) Printed in Great Britain B377

Summary The paper is the second in a series of four which describe a three-year research project into advanced fabric-energy-storage (FES) systems. It presents the construction and validation of a computational-fluid-dynamics (CFD) model of the 'FES-slab' which is subsequently used to investigate the slab's behaviour under a variety of boundary conditions and with modified air paths. Similar models are used to compare the FES-slab with the competing 'generic slab' and 'hollow-core screed' advanced FES systems.

Advanced fabric energy storage II: Computational fluid dynamics modelling

R Winwood†‡ MSc PhD, **R Benstead**† MA MASHRAE and **R Edwards**‡ MSc PhD
†EA Technology, Capenhurst, Chester CH1 6ES, UK
‡University of Manchester Institute of Science and Technology, PO Box 88, Manchester M60 1QD, UK

Received 6 November 1995, in final form 25 June 1996

List of symbols

Ar Archimedes number
COP Coefficient of performance
g Acceleration due to gravity (m s^{-2})
Gr Grashof number
Re Reynolds number
Ri Richardson number
SHC Specific heat capacity (J $kg^{-1}K^{-1}$)
t Time (s)
T Temperature (°C)
v Velocity (m s^{-1})
V Volume (m^3)
V_{eff} Effective volume (m^3)
$\dot{V}$ Volumetric flow rate (m^3 s^{-1})
β Volumetric expansivity of air (1 K^{-1})
δ... Change in ...
Δ... Difference in ...
ρ Density (kg m^{-3})

1 Introduction

An earlier paper[1] reviewed the field of advanced fabric energy storage and introduced the FES-slab, which can be used to damp a building's diurnal temperature swing and reduce its mechanical-cooling and space-heating requirements. This paper details the construction, validation and use of a computational fluid dynamics (CFD) model of the FES-slab.

Some work towards a CFD model of the FES-slab was presented in an earlier paper, in 1993[2]. This model has its origins in that study, but contains a majority of new work.

2 Construction

2.1 *Hardware and software*

The CFD software used for this study was phoenics 1.6.6. Phoenics was chosen as it was the first commercial CFD package (launched in 1981) and is now one of the best validated codes. The hardware was a 66 MHz 486 personal computer with 20 Mb of ram, which is relatively modest power for three-dimensional modelling.

2.2 *Geometry*

The model's geometry was chosen to match the dimensions of a particular 4 m FES-slab which had been investigated experimentally, by the Building Research Establishment[3]. However, as in the preliminary study[2], it was necessary to approximate the geometry of the model's cores to a square cross-section in order to permit the use of a cartesian grid. The cores were defined with their interfacial area (i.e. the perimeter of their cross-section) equal to that of the real, circular cores while the air velocity was adjusted to ensure the correct mass flow rate. The resulting geometry is shown in Figure 1.

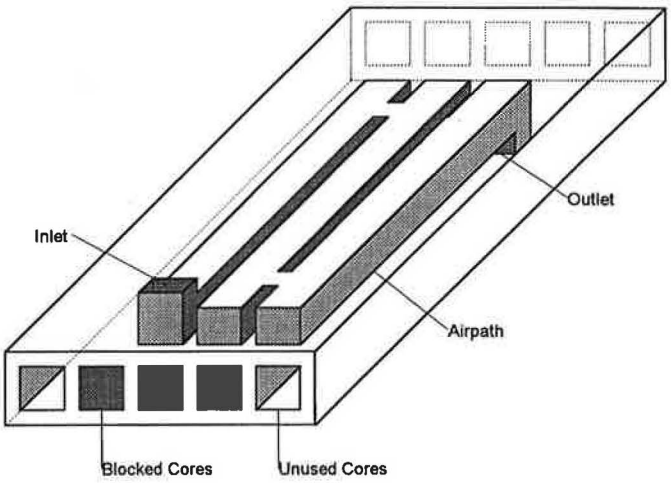

Figure 1 Geometry of the CFD model

2.3 *Turbulence*

Unlike the preliminary model, this simulation was performed using the k–ε turbulence model which allows the evaluation of a local turbulent viscosity, based upon the local flow pattern.

2.4 *Grid and extension to three dimensions*

Normally, the grid of a CFD model would be determined by performing grid-dependence tests on the entire model; however, the large computational requirement made this impractical so an equivalent two-dimensional slice was investigated, as shown in Figure 2. It was defined with a 100 W m^{-1} heat flux around the perimeter and an air supply at 1 m s^{-1} and 0°C.

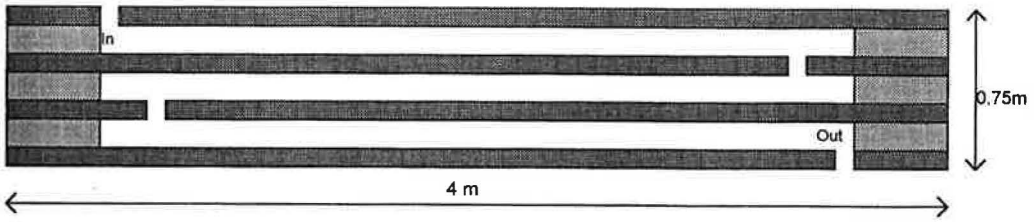

Figure 2 Two-dimensional slice used for grid-dependence tests

The number and spacing of the model's cells was varied until further grid refinement produced no change in the average outlet temperature, the field maximum and minimum pressures or the temperature or pressure profiles along the central core. For the average outlet temperature it was possible to compare the model with the analytical solution below, which was calculated from an energy balance.

$$T_{out} = 6.4°C \quad (1)$$

The model produced an average outlet temperature of 6.3°C, suggesting an accuracy of ± 0.1°C (which is better than would normally be expected from a thermocouple).

Figure 3 shows the extension of the model into three dimensions, producing a grid which contained 67 × 19 × 69 ≈ 90 000 cells.

2.5 *Selection of the time step*

Analysis of the Building Research Establishment's experimental data showed that a 15 minute time step was likely to produce a change of between 0.10°C and 0.15°C in the slab temperature. This was considered acceptable, so time was initially discretised into 15 minute intervals.

2.6 *Physical properties*

In reality, the physical properties of air are dependent on temperature, pressure and moisture content. Simulating these dependencies would have increased greatly the time required to converge a solution, so the model was defined with the constant properties listed in Table 1. It was therefore possible to solve a steady-state flow field and then solve the time-dependent temperature field by superimposition upon it.

Defining air with constant physical properties necessitated the omission of free convection from the model. Its significance was estimated through the evaluation of the Richardson number[4] and the Archimedes number[5]:

Table 1 Physical properties assigned to the models

Material	Density(kg m^{-3})	Conductivity (W m^{-2}K^{-1})	Specific heat capacity (J kg^{-1}K^{-1})
Precast FES-slab concrete	2432	1.9	781
Screed	1200	0.38	1000
Air	1.2	0.026	1008

The Richardson number is defined by equation 2:

$$Ri = g\beta \Delta T \Delta L / \Delta v^2 \quad (2)$$

where ΔL represents a typical length scale and ΔT and Δv are the associated temperature and velocity scales. Substitution of values appropriate for a FES-slab duct produced the result Ri = 0.06.

The Archimedes number is defined as:

$$Ar = Gr/Re^2 \quad (3)$$

Evaluation with FES-slab dimensions yielded Ar = 1.6 × 10^{-3}.

It is generally accepted that buoyant effects can be ignored once Ri < 0.1 or Ar > 10. Comparison with the FES-slab values confirmed that the omission of free convection was unlikely to affect the model.

2.7 *Boundary conditions*

The following boundary conditions were defined at the model's exterior surfaces. Most of the conditions were entered directly into the model definition file, although the more complex conditions, particularly those involving time dependence, required modification of the PHOENICS source code.

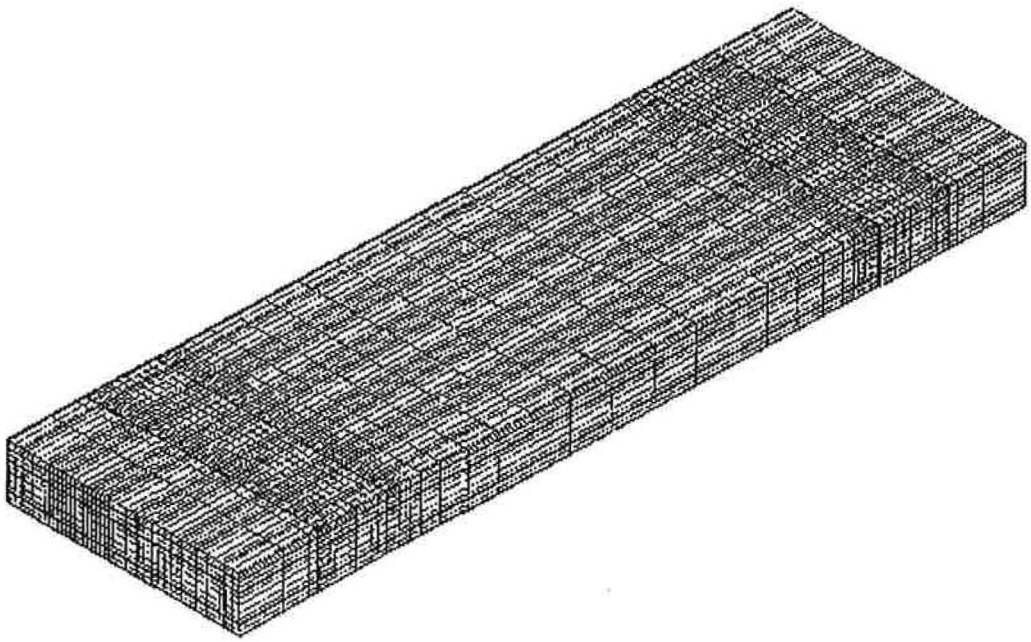

Figure 3 Grid structure of the three-dimensional CFD model

The inlet boundary conditions ensured an air-flow rate of 20 l s^{-1}, as in the Building Research Establishment experimental study. The inlet velocity was therefore defined as 1.13 m s^{-1}, while the values of all other variables were derived from the velocity.

The incoming air was defined to be 2% turbulent (i.e. its turbulent energy was 2% of the incoming kinetic energy — the PHOENICS default setting), while its temperature was read from an external data file.

A cyclic boundary condition simulated the presence of identical slabs adjoining each side of the model, while heat exchange due to radiation and free convection at the top and bottom surfaces was evaluated according to the procedure illustrated in Figure 4.

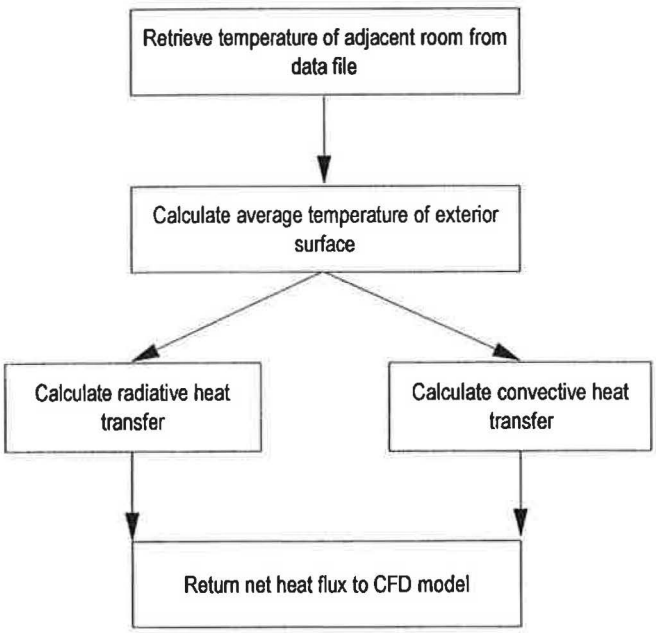

Figure 4 Evaluation procedure for external heat fluxes

Free convective heat transfer was calculated according to the formulae of the *CIBSE Guide*[6], with the exception of downwards free convection, which was set to zero to mimic the effect of thermal buoyancy within an enclosed space. Radiative heat transfer was calculated according to the Stefan–Boltzmann law, with the assumptions that the spaces around the slab behaved as black bodies with mean radiative temperatures equal to the respective air temperatures.

2.8 Output data

The model recorded the values of key parameters at the end of each time step, including:

Tout: the temperature of air leaving the slab. This was approximated to the temperature at one particular cell within the outlet, which was chosen as it represented the greatest rate of mass flow out of the model.

Tslab: the average slab bulk temperature. This was approximated to the temperature within a single cell at the centre of the fourth concrete pier. The position was selected to correspond with the average positioning of the mass temperature sensors used in the Building Research Establishment experimental study.

3 Validation

Validation of the model was performed against the Building Research Establishment's experimental data. Unfortunately, the model's steady-state flow field meant that it was only possible to compare it with periods of continuous fan operation. Three validation periods were therefore selected according to the following criteria:

(*a*) They involved relatively long periods of uninterrupted operation. Long periods were required in order to provide a meaningful evaluation of the model.

(*b*) They followed intervals with relatively stable slab mass temperatures. Unfortunately, it was necessary to initialise the model with a uniform temperature. This would have been closest to experimental conditions after a long stable period, when thermal conduction would have minimised any local temperature gradients.

(*c*) The values of T_{in}, T_{hall} and T_{room} all varied smoothly throughout the validation period. A sharp variation in these parameters would have required a reduction in the simulation's time step or a corresponding loss of definition in the temperature profile.

3.1 Initialisation of the slab

The model was initialised with the temperature of the experimental data at the start of the first time step. This initialisation, with the entire slab at a uniform temperature, is acknowledged as flawed; however, there was no alternative.

The CFD model was compared with experiment in terms of two key parameters: the temperature of air as it left the slab and the temperature of the slab bulk. Results from the first validation are illustrated in Figures 5 and 6, while results from all three validation periods are summarised in Table 2, where the average disagreement between the CFD results and experimental data was calculated according to equation 4:

$$\text{Average disagreement} = 100\% \times |(T_{\text{simulated}} - T_{\text{experimental}})/T_{\text{experimental}}| \quad (4)$$

To ensure that the results were independent of the time interval, the first validation was repeated with a 5 minute time step; however, there was no significant improvement so the 15 minute time step was carried forwards to all subsequent models. Time steps greater than 15 minutes were not investigated as it was felt that they would produce excessive smoothing of the time-dependent boundary conditions.

Table 2 Average disagreement during validation periods

Validation period	Average disagreement in T_{slab} (%)	Average disagreement in T_{out} (%)
1	2.3	1.8
2	2.7	2.0
3	2.6	2.0

4 Specification of a standard test

Once a model of the FES-slab had been constructed and validated, it was necessary to devise a standard test procedure which would permit a fair comparison between subsequent models.

4.1 Selection of period

It was important to ensure that the standard test involved the simulation of an interval long enough for the model to

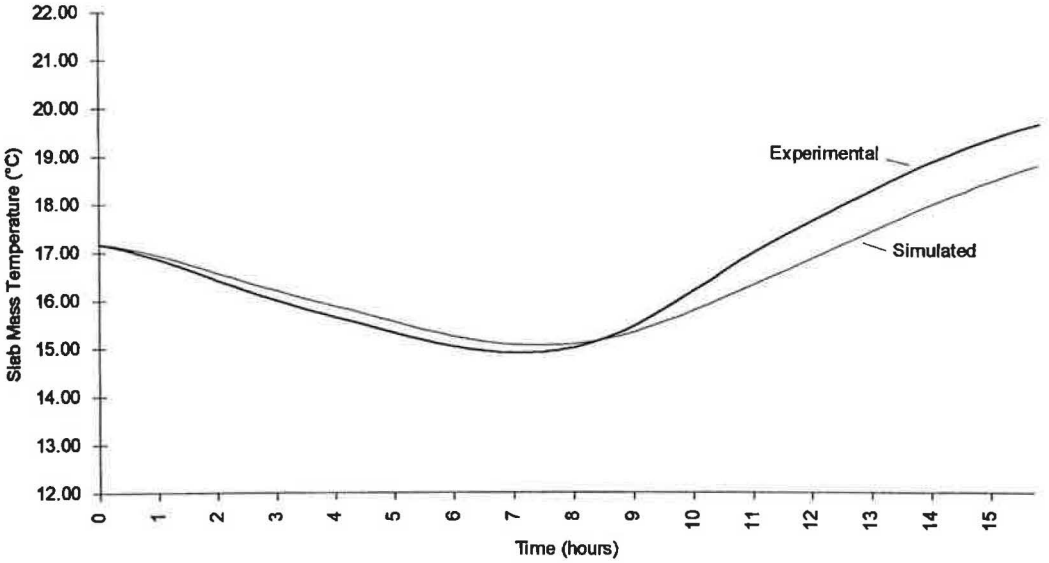

Figure 5 Slab mass temperatures recorded during validation period 1

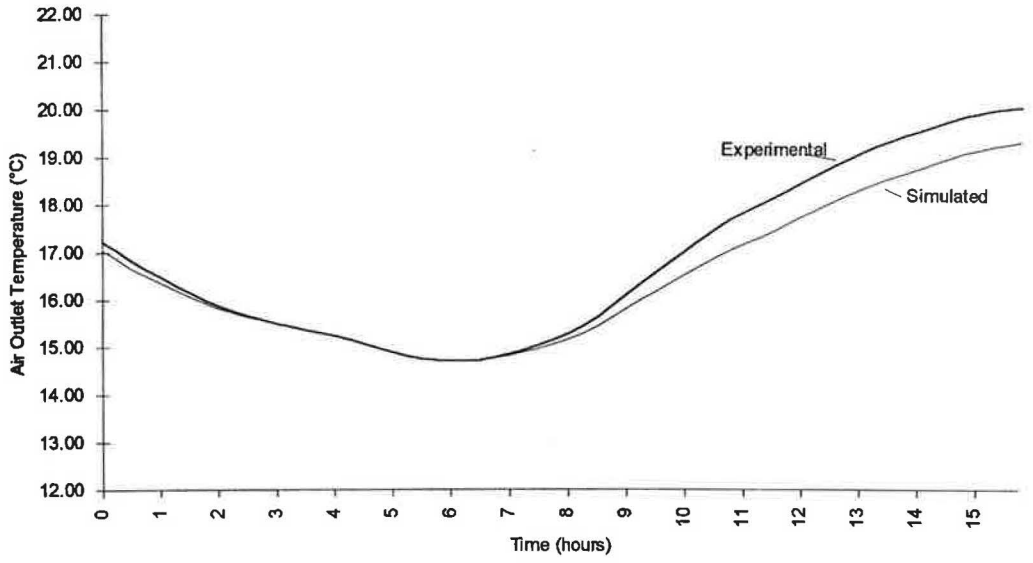

Figure 6 Outlet temperatures recorded during validation period 1

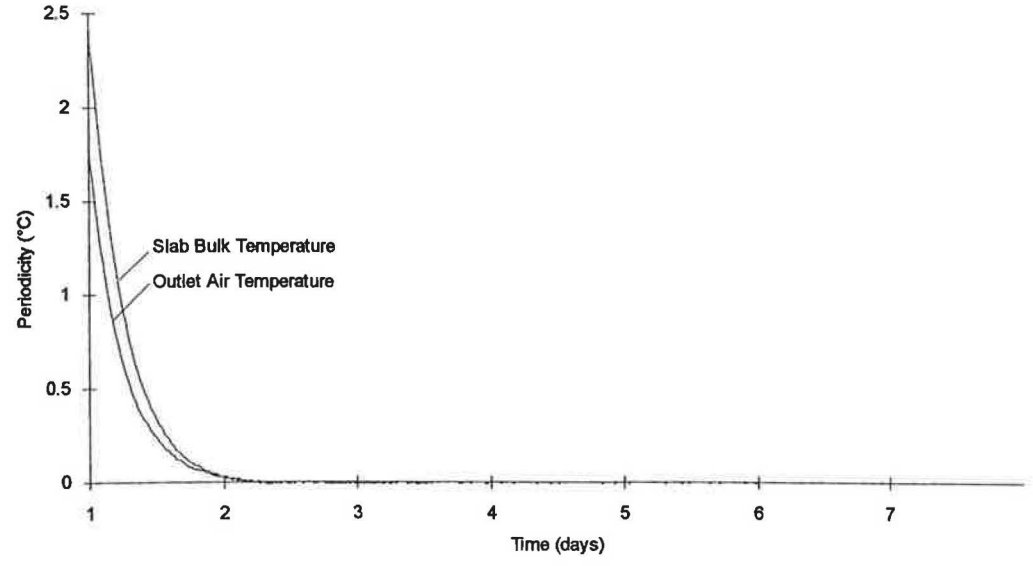

Figure 7 Periodicity versus time

become periodic and its results to become independent of the 'end effect' of the uniform slab-initialisation temperature. A week-long simulation was therefore performed and the results analysed according to equation 5, to produce Figure 7:

$$\text{Periodicity} = T(t_0) - T(t_0 + 24\text{ h}) \quad (5)$$

The figure shows that, within 0.03°C, the model became periodic after one day. The standard test was therefore defined

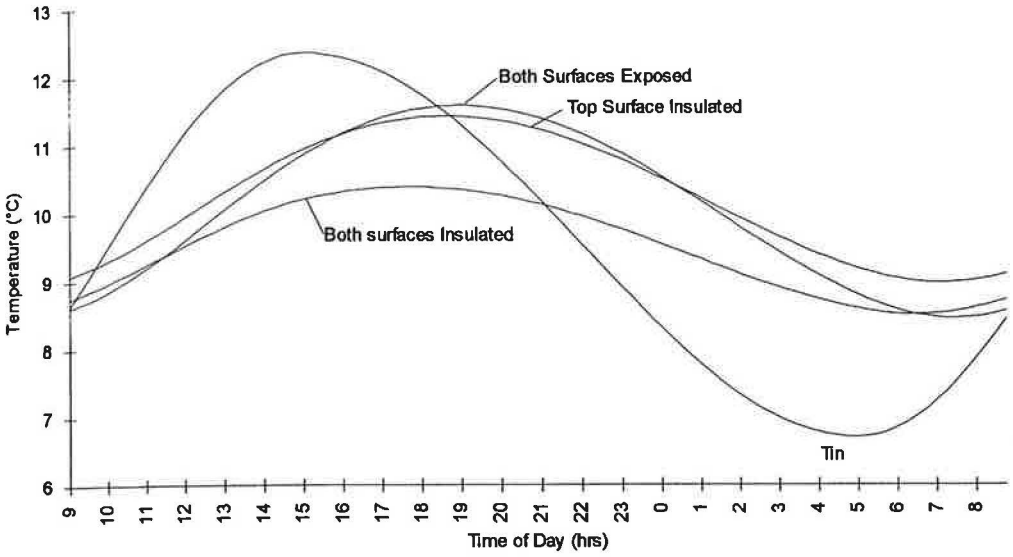

Figure 12 Diurnal temperature profiles with varying insulation

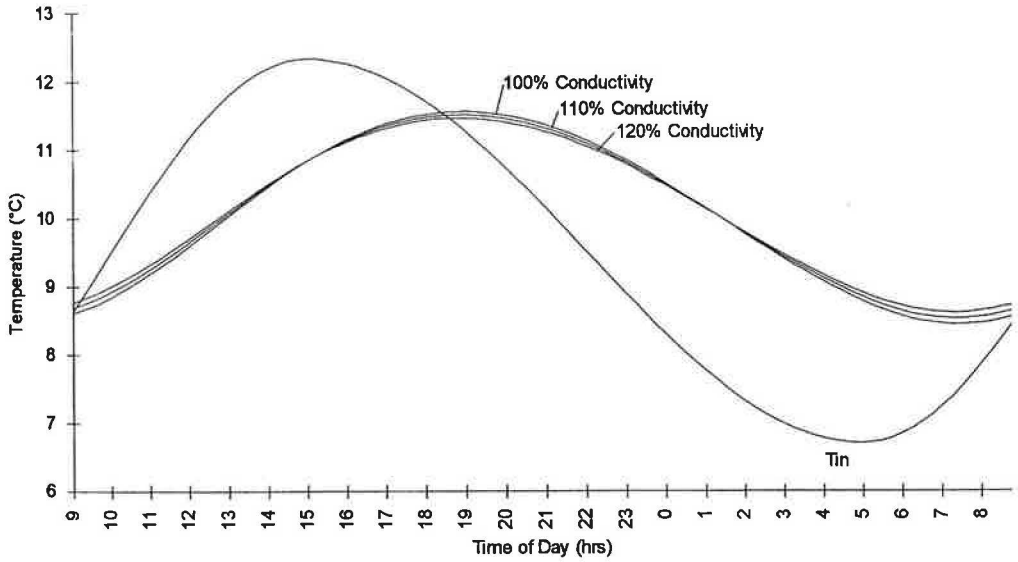

Figure 13 Diurnal temperature profiles with varying thermal conductivities

is independent of the flow rate, a simple analysis shows that the internal energy transfer will behave according to

$$\text{Internal heat transfer} \propto V' \quad (8)$$

The fan laws[11], however, show that the energy expended in maintaining the air flow varies according to

$$\text{Energy expended} \propto V'^3 \quad (9)$$

If the system's coefficient of performance is defined as the ratio of useful energy transfer to expended energy, equations 8 and 9 may be combined to give equation 10:

$$\text{COP} \propto 1/V'^2 \quad (10)$$

This indicates that the system is most efficient when supplying the minimum sufficient air volume and that it quickly becomes less efficient at higher flow rates.

The effect of different air supply rates was further investigated by simulating flows of 5, 10, 20 and 30 l s^{-1}, producing the outlet air temperature profiles shown in Figure 14. The profiles illustrate the slab's increasing thermal stability at lower flow rates, as quantified by the increasing effective volumes in Table 4.

Table 4 also shows that the CFD models reproduced the expected trend of reduced storage efficiency at higher flow rates, owing to the reduction in the transit time for air to pass through the slab. This effect compounds the variation of the slab's COP with ventilation rate, as defined in equation 10, and increases the importance of avoiding unnecessarily high flow rates.

Table 4 FES-slab with varying flow rate

Flow rate (l s^{-1})	5	10	20	30
Effective volume (m^3)	0.9	0.7	0.6	0.5
Intrinsic storage efficiency (%)	97.5	90.6	77.6	70.8

8 FES-slab variant models

Once the standard FES-slab had been investigated, models were constructed to study two alternative air paths; switchflow and five-core operation.

The switchflow model simulated one-core operation, with the new inlet positioned 60 cm downstream of the last corner in the three-core air path, as in the Building Research Establishment's experimental study. The five-core model used two interconnected air paths, as shown in Figure 15.

Figure 16 compares the outlet-air-temperature profiles produced with the different air paths. It shows that, as expected,

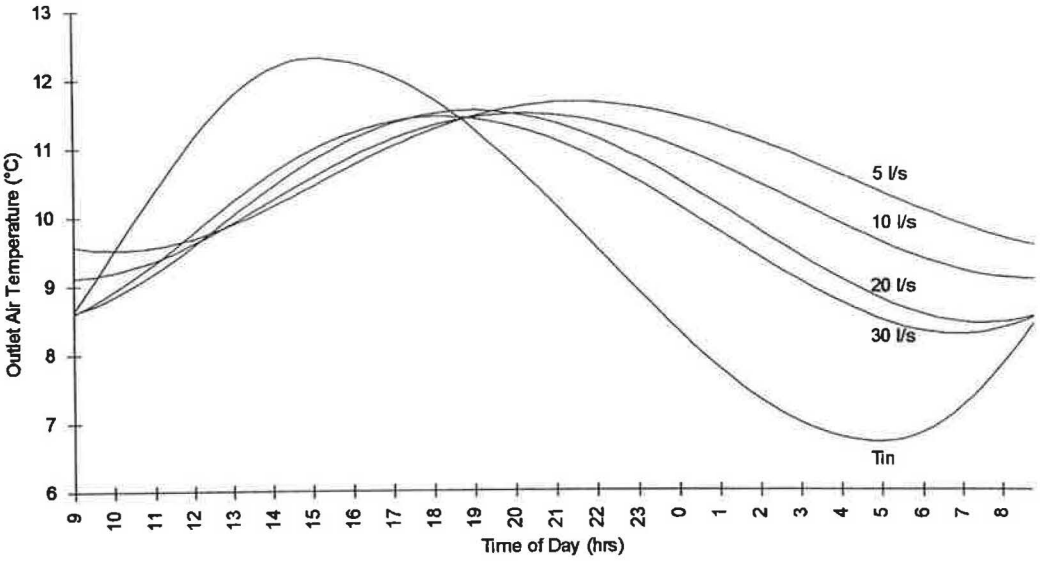

Figure 14 Diurnal temperature profiles with varying flow rates

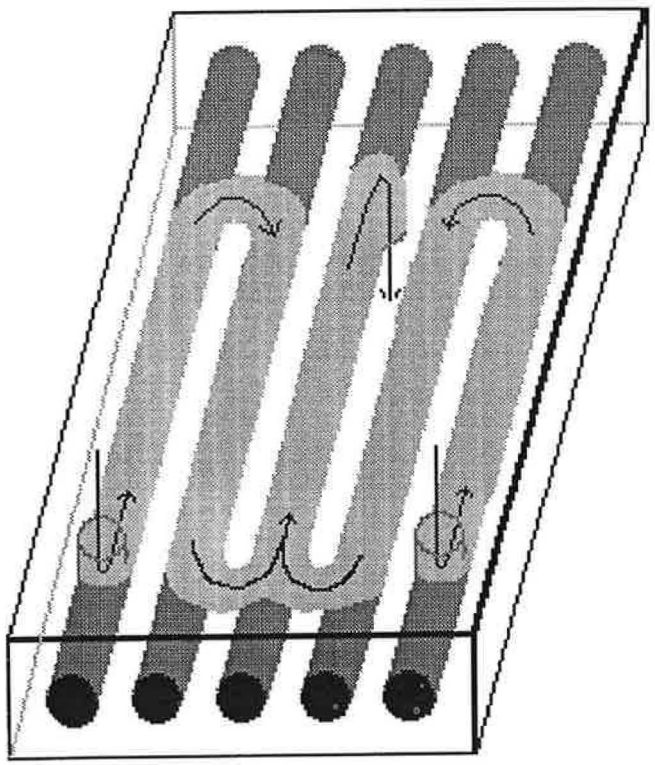

Figure 15 The five-core FES-slab

Table 5 FES-slab variants

FES-slab model	Switchflow	Three-core	Five-core
Effective volume (m^3)	0.5	0.6	0.8
Intrinsic storage efficiency (%)	35.1	77.6	89.3

the greater the proportion of the slab that was linked to the interaction, the smoother was the diurnal temperature profile. Table 5 quantifies this effect on the slabs' effective volumes and intrinsic storage efficiencies.

The improved storage efficiency and an increased effective volume of the five-core slab combine to make it the most effective of the variants, although it is not clear whether this improved performance would merit the increased capital cost of the additional holes in the slab and the associated reduction its structural integrity.

9 Alternative systems

Further models simulated the generic slab and the hollow-core screed, providing the first chance to compare the FES-slab quantitatively with these competing systems. As far as possible, the additional models were similar to the FES-slab model, being 4 m long with the air-supply rate defined to ensure that each system provided 20 l s^{-1} of air flow for every 1.2 m of slab width.

Generic slab models were constructed with two active cores, as at the Ionica building, and with all three central cores active, as in the FES-slab.

The hollow-screed model, unfortunately, had to be simplified by the omission of the cores from the slab beneath the screed. This was expected to have a limited effect on the slab's performance as the cores are in the least active, central region of the slab.

Figure 17 shows the outlet air temperature profiles produced by the different systems while Table 6 quantifies their performance. The table shows that both generic slabs were inferior to the FES-slab although, as expected, the generic slab's performance did improve when three cores were used. The hollow screed was found to produce an excellent level of heat transfer and a very stable slab outlet air temperature; however, it must be borne in mind that its high effective volume may have been due to the model's omission of the hollow cores of the supporting slab.

The CFD model presented the first opportunity to study the air-flow pattern within the hollow core screed, as shown in Figure 18. The figure indicates that the interconnections between parallel cores have little effect upon the air-flow pattern, suggesting that it may be possible to omit them with little reduction in performance.

10 Varying slab lengths

As the slabs in a real building are likely to be considerably longer than the 4 m slabs simulated in the bulk of this project, FES-slabs and three-core generic slabs of 6 m and 8 m length were added to the existing 4 m models. Unfortunately, the high computational requirement made it impractical to simulate further increases in length. All of the longer models retained the general form of the original 4 m slab, although